Electronic Supplementary Material (ESI) for ChemComm.

Electronic Supporting Information

Efficient Kinetic Separation of Propene and Propane by Two Microporous Metal Organic Frameworks

Junjie Peng,[a,b] Hao Wang,[b] David H. Olson,[b] Zhong Li[a] and Jing Li*[b]

[a] Department of Chemistry and Chemical Engineering, South China University of Technology, Guangzhou, 510640, China.

[b] Department of Chemistry and Chemical Biology, Rutgers University, Piscataway, New Jersey, 08854, USA.

E-mail: jingli@rutgers.edu

S1. Material Preparation

Materials. All reagents used were purchased from Alfa Aesar, Fisher Scientific and used without purification.

Synthesis of $Zn(ox)_{0.5}(trz)$ (1) and $Zn(ox)_{0.5}(atrz)$ (2). The preparation was followed by a reported method with minor modifications.[1] Zinc carbonate, oxalic acid and 1,2,4-triazole in the ratio of 1:1:5 were added to binary solvent of 3mL BuOH and 3mL H_2O in a 23mL autoclave. The slurry was stirred for 1 hour at room temperature, and then heated for 180°C for 3 days. After cooled to RT, the resultant powder was filtered, washed thoroughly with water and methanol and dried under air. Similar procedure was employed to preparation of Zn(ox)0.5(atrz) with replacing 1,2,4-triazole with 3-amino-1,2,4-triazole.

S2. Characterization Details

Powder X-ray diffraction analysis (PXRD). All PXRD patterns were performed on a Rigaku Ultima IV automated diffractometer. Data were collected between 3° and 40° of 2θ with a scan speed of 2.0 deg/min.

Thermal analysis (TA). Thermogravimetric data were recorded on a TA Q5000 Analyzer with a temperature ramping rate of 10K/min from RT to 873 K under nitrogen atmosphere.

Helium simulation. Size and shape of the pores of adsorbents are the key factors for kinetic separation. Often a single crystal structure drawing does not clearly show the detailed pore structure (e.g. shape and size). Helium adsorption simulation gives a clear and detailed outline of the pore geometry and size. Therefore, it was carried out in this study.[2]

Adsorption isotherm experiment. CO_2 adsorption experiments at 195 K were performed in a dry ice-acetone bath using a volumetric gas sorption analyzer (Autosorb-1 MP, Quantachrome Instruments). C3 isotherms were tested on the same instrument while the temperatures were controlled by using a water bath. The free space of the system was obtained by dozing the helium gas. Before each measurement, about 100 mg sample was degassed at 423 K in vacuum for 10 h.

Propene and propane adsorption measurements. Time dependent adsorption measurement of propene and propane were carried out on a computer controlled thermogravimetric balance with a TA51 electrobalance and associated TA-2000/PC control system. The gas flow through electrobalance system was controlled via Macintosh-based LabView control software, Kinetic Systems interface, mass flow controllers and Eurotherm temperature controller. Nitrogen was used as the inert gas and the volume ratio of the gaseous of mixtures was 6/1 (C_3H_6/N_2 and C_3H_8/N_2). Adsorption rate measurements were done at a partial pressure of 650 Torr, at which the adsorption reached saturation based the adsorption isotherm results. The samples were activated at 473 K for 2 h in nitrogen before each sorption measurement.

S3. Crystal Structures

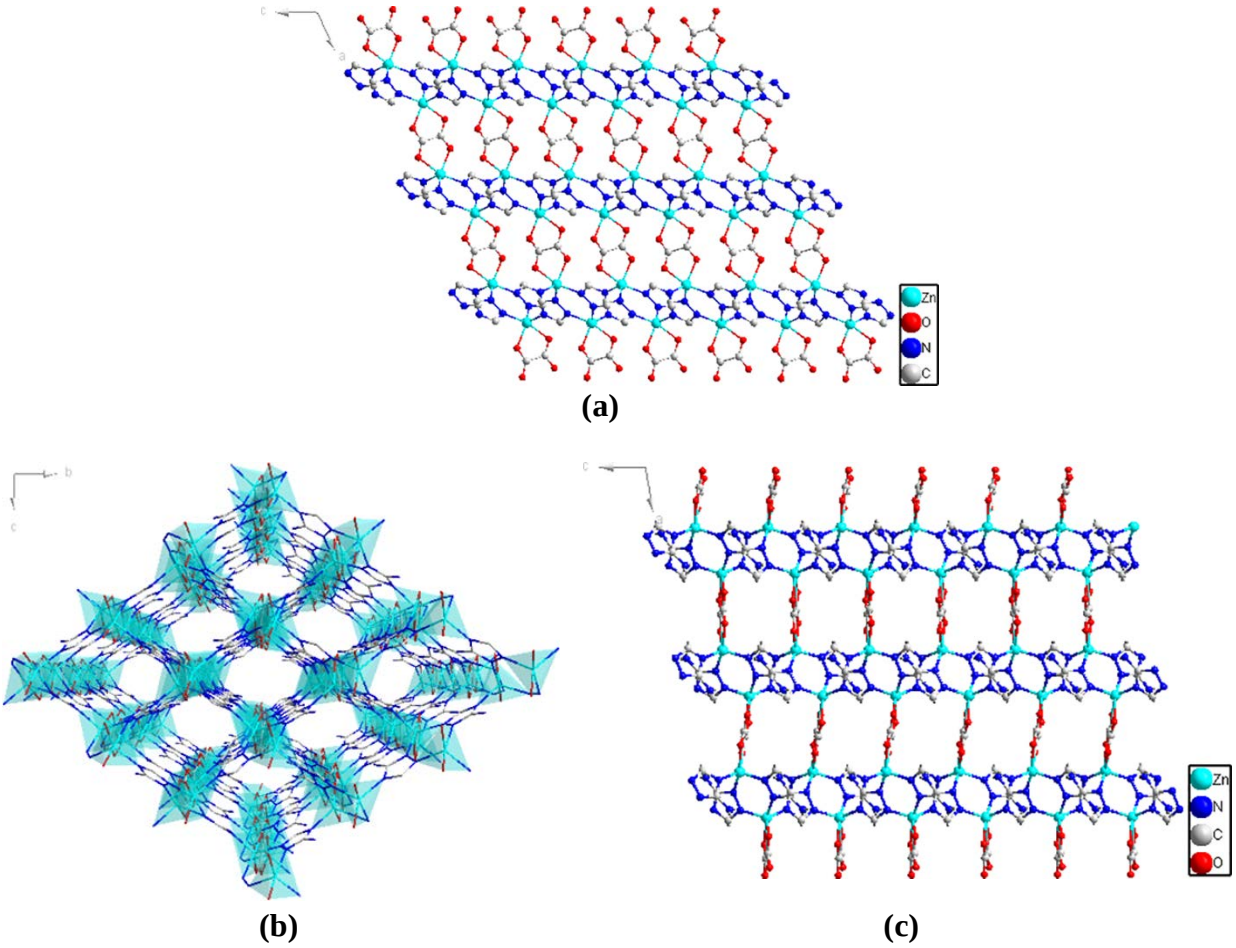

Fig. S1. (a) View of the crystal structure of compound **1** along the *b* axis. (b) View of the crystal structure of compound **2** along the *a* axis. (c) View of the crystal structure of compound **2** along the *b* axis.

S4. PXRD Analysis

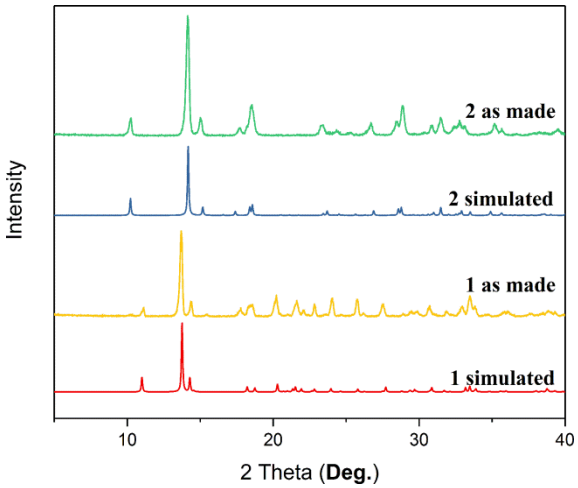

Fig. S2. PXRD patterns of compounds **1** and **2**, along with simulated patterns based on single crystal data.

S5. Thermogravimetric Analysis (TGA)

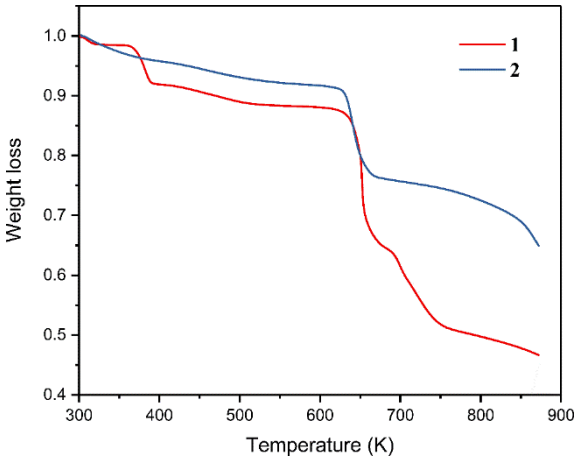

Fig. S3. TGA data for Compounds **1** and **2**.

S6. CO_2 Adsorption Isotherms.

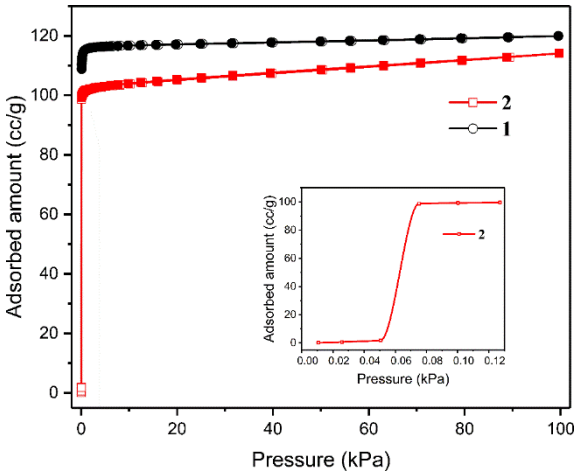

Fig. S4. CO_2 adsorption isotherms of **1** and **2** at 195 K (Open and close symbols represent the adsorption and desorption branches, respectively). Inset: CO_2 adsorption data of **2** at 195 K and low pressure range.

S7. Thermal and Water Stability Analysis.

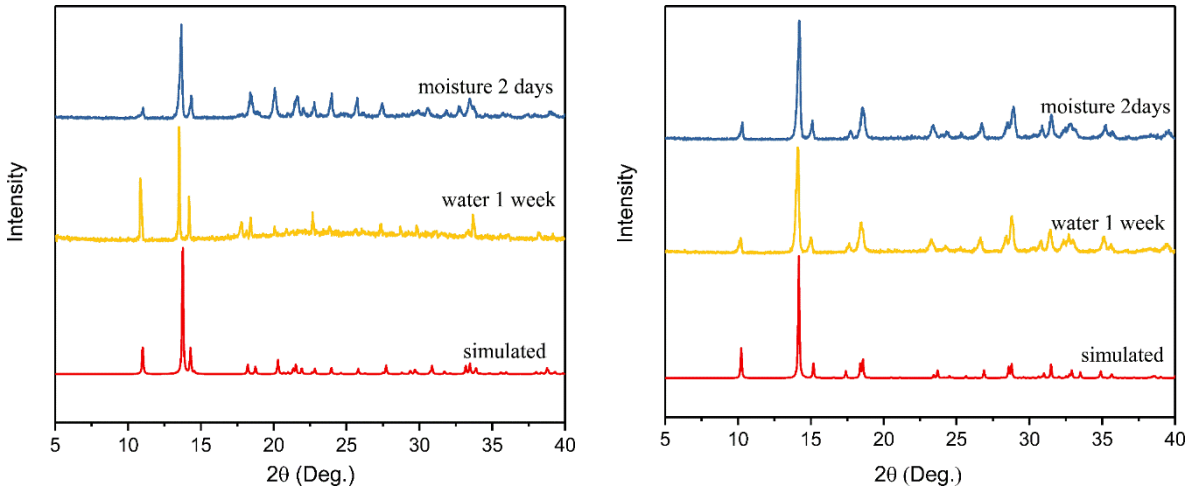

Fig. S5. Thermal and water stability analysis of **1** (left) and **2** (right) under various conditions at room temperature.

S8. Propene Adsorption Analysis

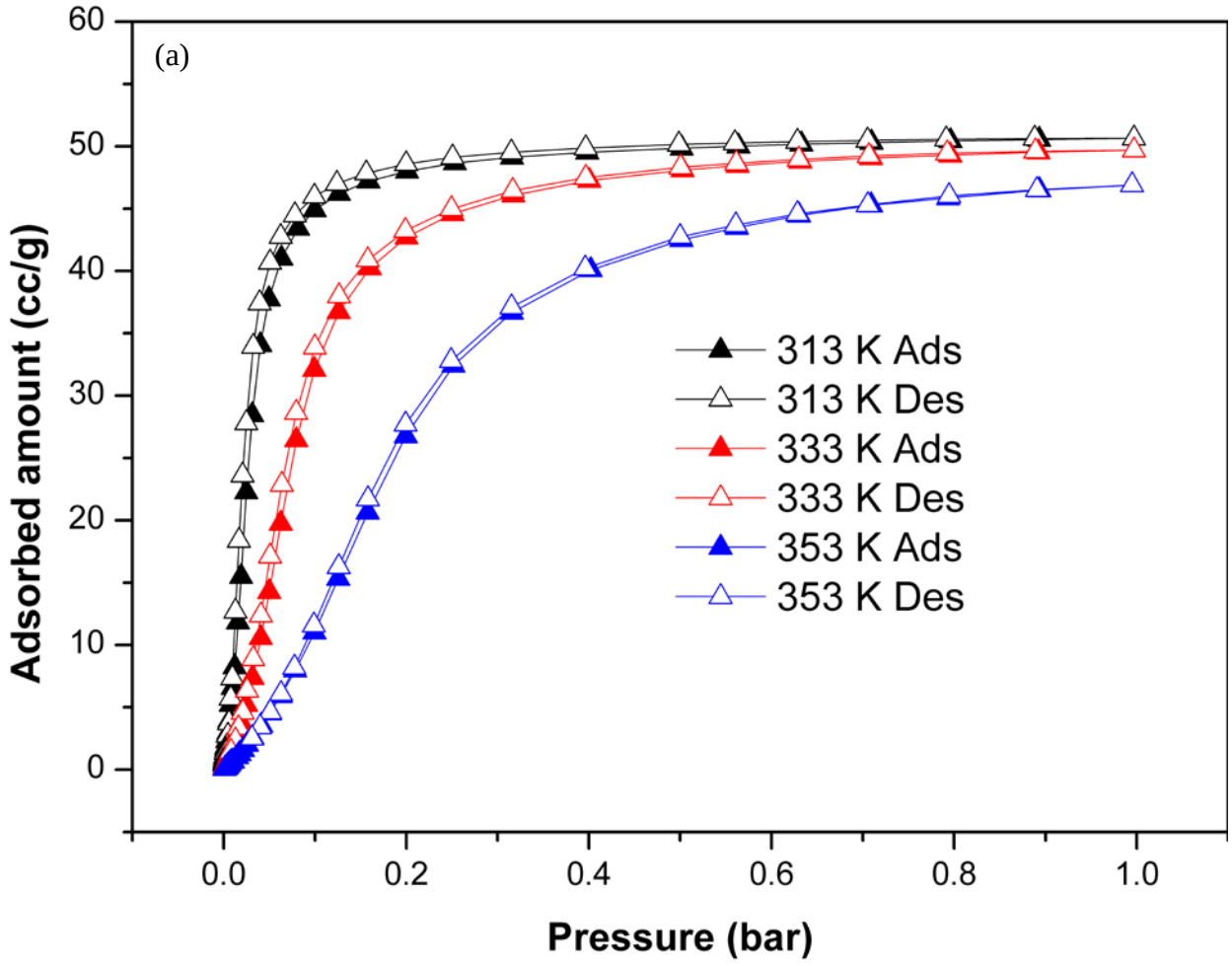

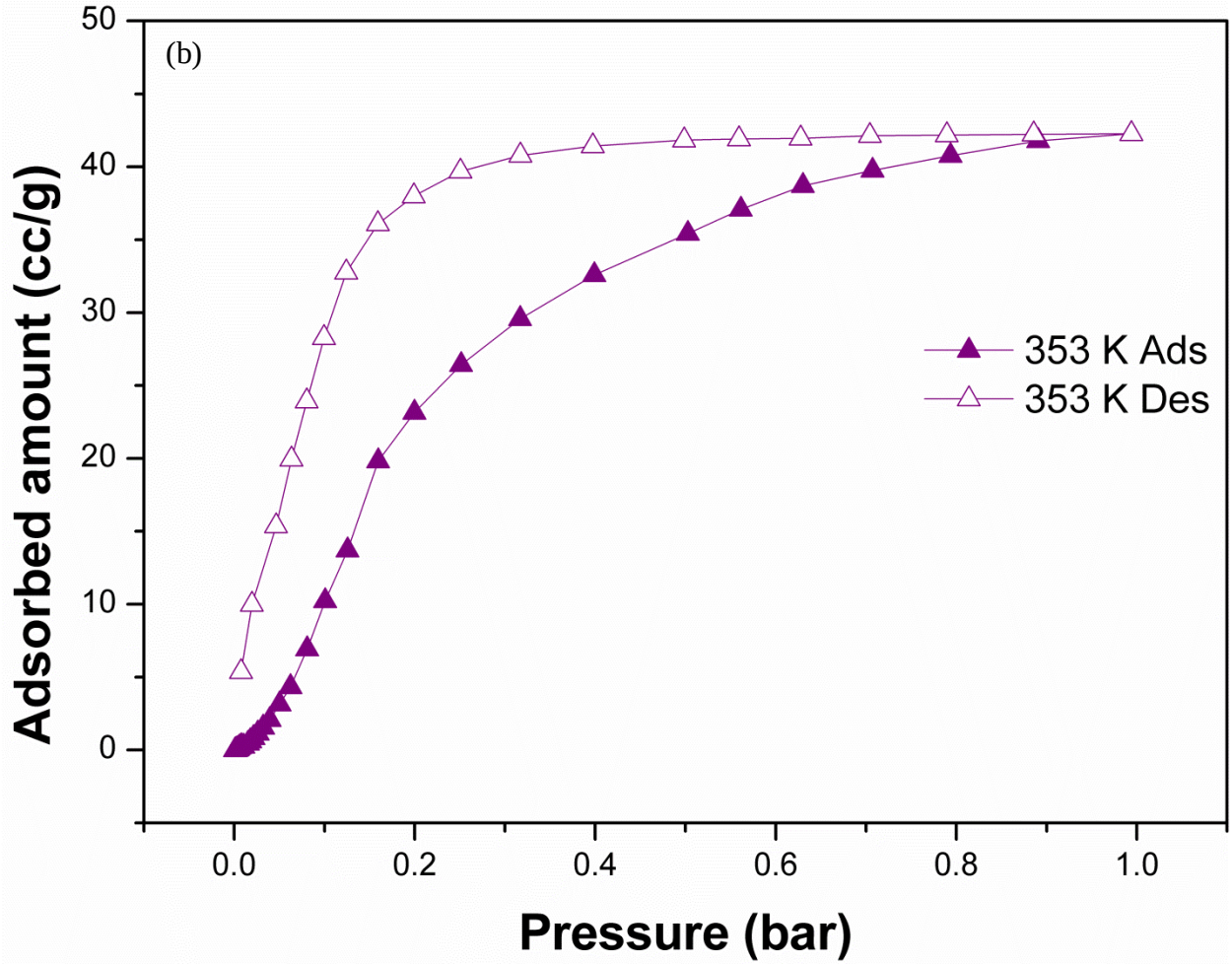

Fig. S6. (a) Propene adsorption isotherms of **1** at different temperatures. (b) Propane adsorption isotherm at 80 °C.

S9. Isosteric Heat for Propene

Isosteric heat of propene adsorption on compound **1** has been calculated using adsorption isotherms at different temperatures (313 K, 333 K, and 353 K) with virial method.[3] The isotherms were first fitted with Virial equation.

$$\ln(p) = \ln(v) + (1/T)\sum_{i=0}^{m} a_i v^i + \sum_{j=0}^{n} b_j v^j$$

Where p is pressure, v is amount adsorbed; T is temperature and a_i, b_j are empirical parameters which are independent of temperature.

Isosteric heat of adsorption can then be calculated by the equation below.

$$Q_{st} = -R\sum_{i=0}^{m} a_i v^i$$

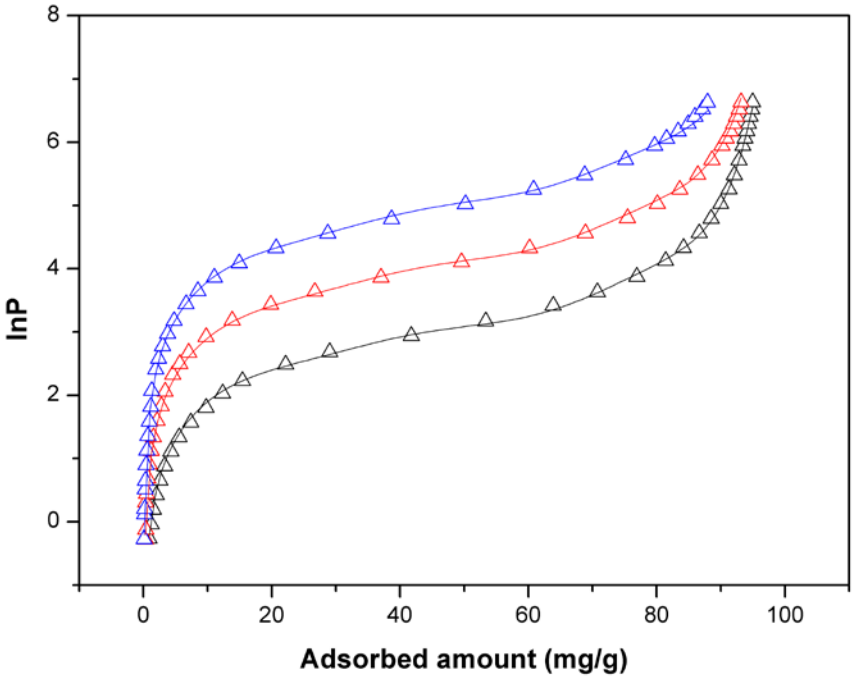

Fig. S7. Virial fitting of propene adsorption isotherms at 313 K (black), 333 K (red), and 353 K (blue). Symbols and lines represent experimental and fitted data, respectively.

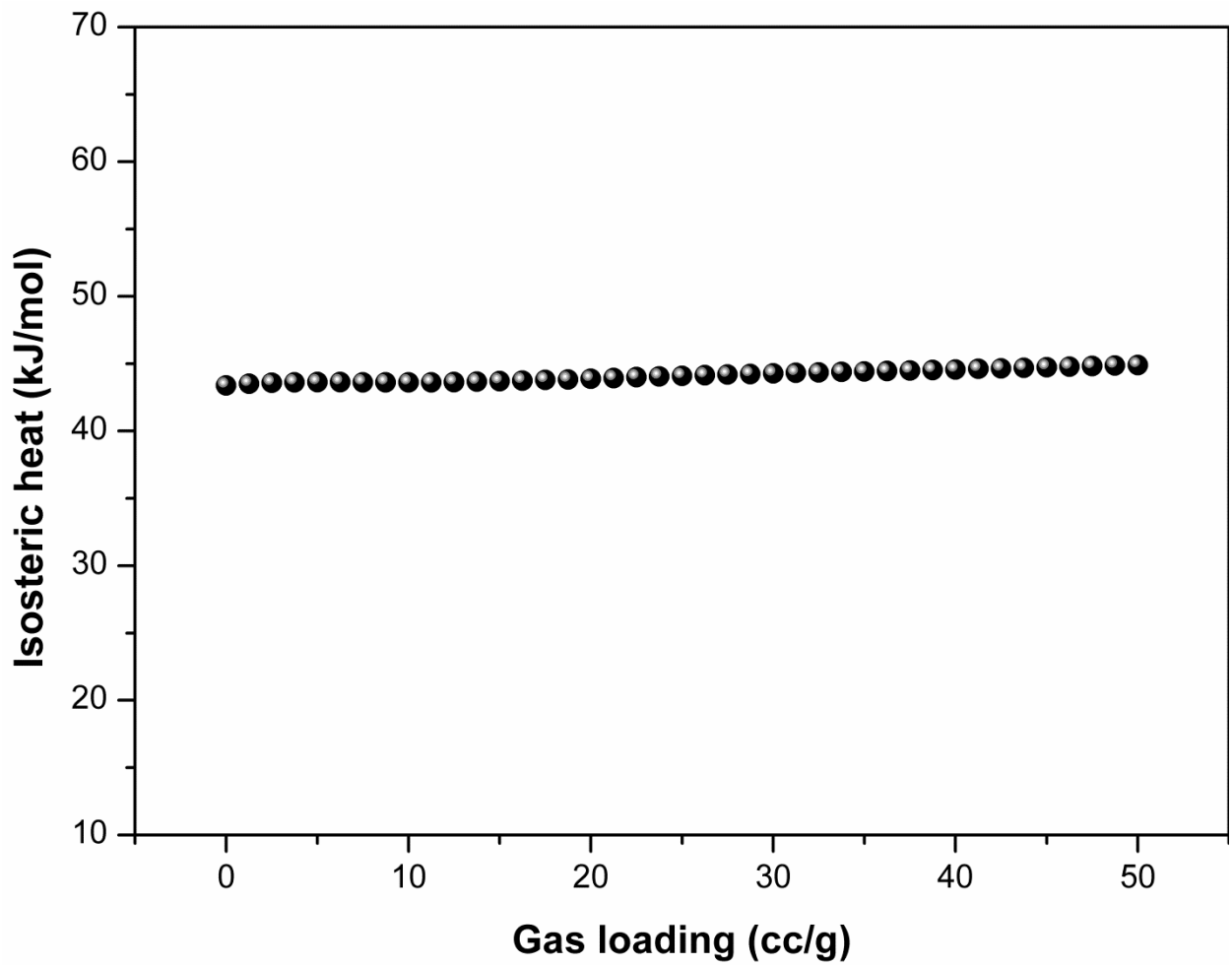

Fig. S8. Isosteric heat as a function of propene loading for compound **1**.

S10. Kinetic Selectivity and Equilibrium Uptake of Propane and Propene.

Diffusional time constants (D', D/r^2) were obtained from the short-time solution of the diffusion equation presuming a s step change in the gas-phase concentration, micropore diffusion control and clean beds initially:[3]

$$\frac{q_t}{q_\infty} = \frac{6}{\sqrt{\pi}} \cdot \sqrt{\frac{D}{r^2} \cdot t} \qquad (3)$$

Where q_t is the gas uptake at time t, q_∞ is the gas uptake at equilibrium, D is the diffusivity and r is the radius of the equivalent spherical particle. Therefore, the slopes of q_t/q_∞ versus $\sqrt{t}$ are derived from the fitting of the plots in the low gas uptake range, and then D' can be obtained from the square of the slope multiplying by $\pi/36$.

Fitting of q_t/q_∞ versus $\sqrt{t}$ in compound 1

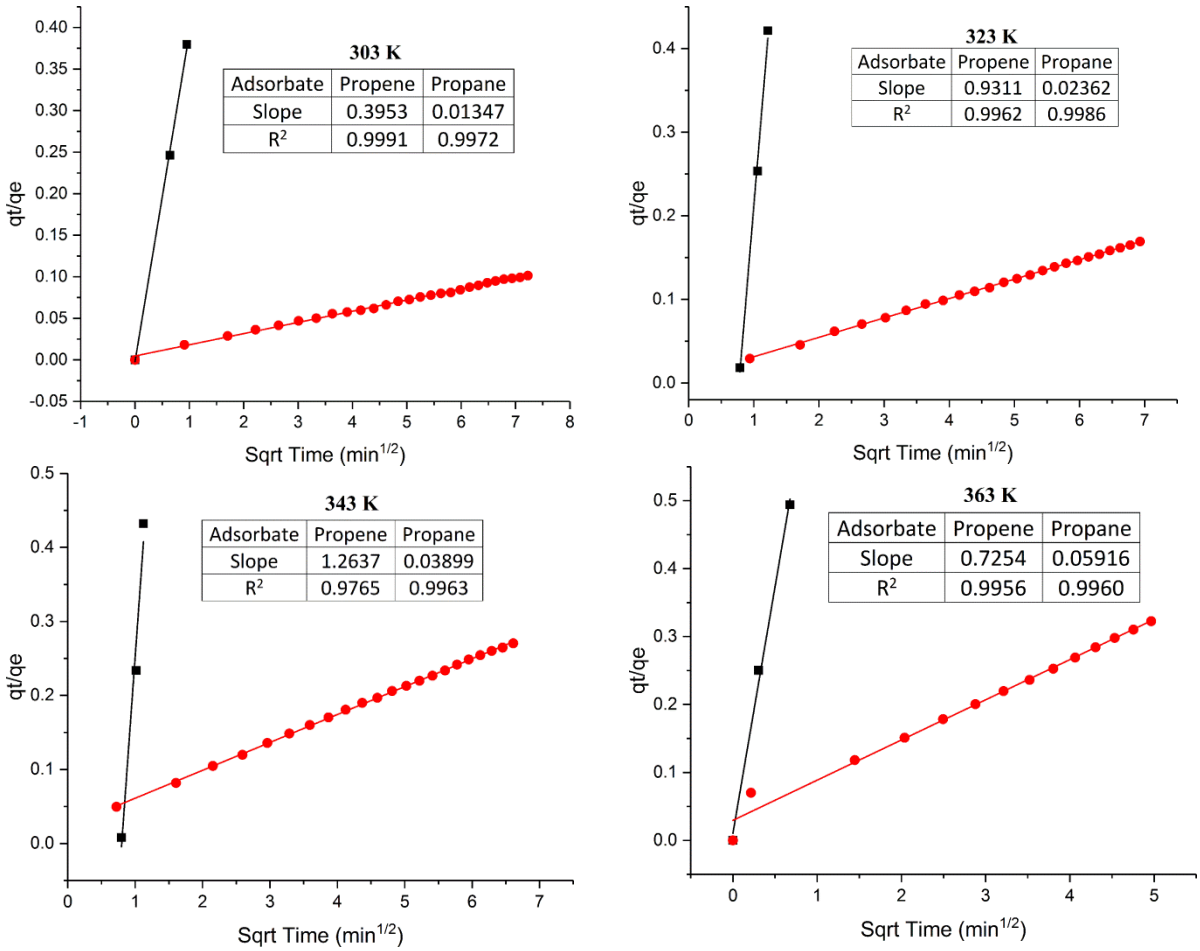

Fig. S9. diffusional time constant calculation details for compound **1**. Square and circle symbols represent propene and propane, respectively.

Fitting of q_t/q_∞ versus $\sqrt{t}$ in compound 2

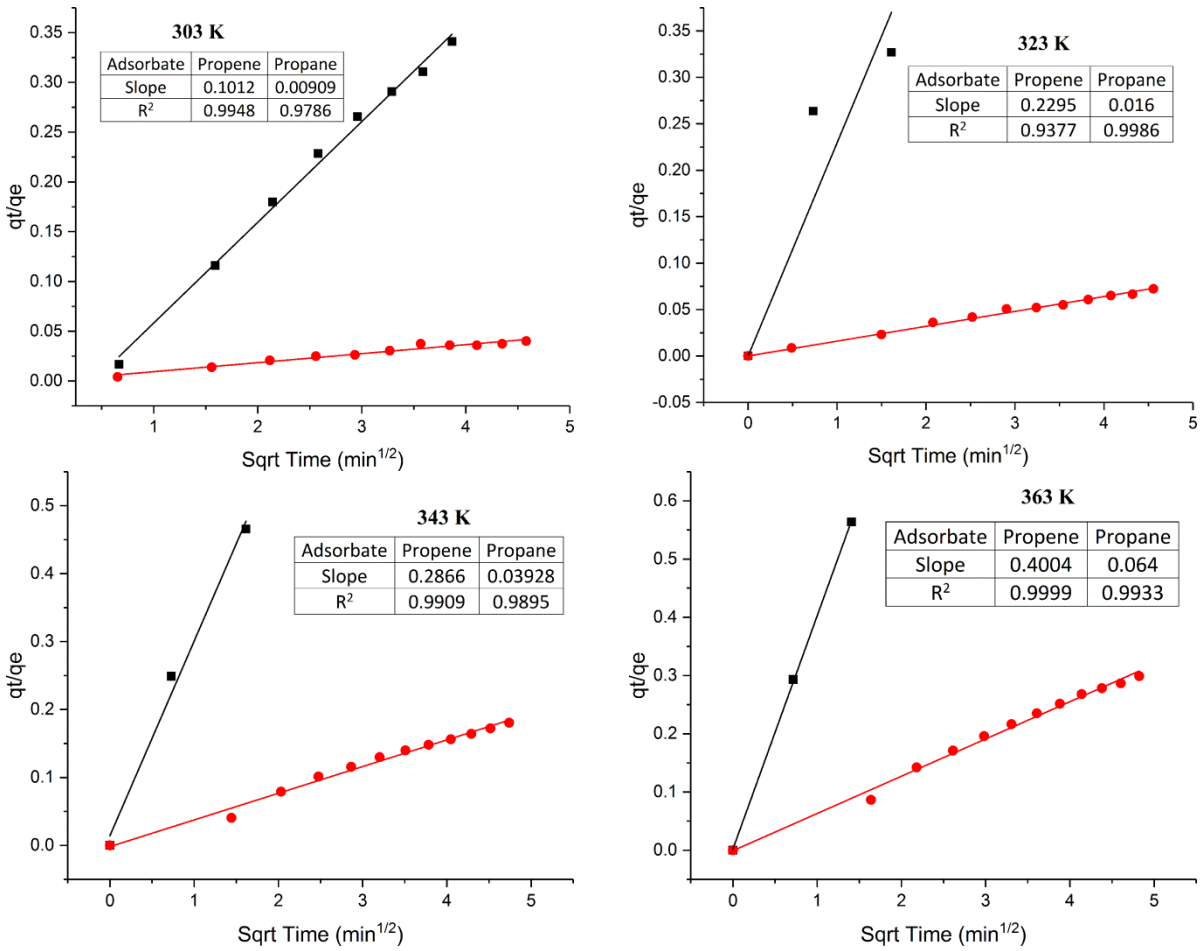

Fig. S10. diffusional time constant calculation details for compound **2**. Square and circle symbols represent propene and propane, respectively.

Table S2. Diffusional time constants (D') and kinetic selectivity on **1** and **2**.

Material	Temperature (K)	D' (propene, min^{-1})	D' (propane, min^{-1})	Kinetic selectivity
1	303	$1.35x10^{-2}$	$1.57\ x10^{-5}$	860
	323	$7.48\ x10^{-2}$	$4.78\ x10^{-5}$	1565
	343	$1.39\ x10^{-1}$	$1.32\ x10^{-4}$	1051
	363	$4.39\ x10^{-2}$	$2.92\ x10^{-4}$	150
2	303	$7.73\ x10^{-4}$	$4.41\ x10^{-6}$	175
	323	$4.58\ x10^{-3}$	$2.08\ x10^{-5}$	220
	343	$7.70\ x10^{-3}$	$1.32\ x10^{-4}$	58

	363	1.92 x10^{-2}	3.86 x10^{-4}	50

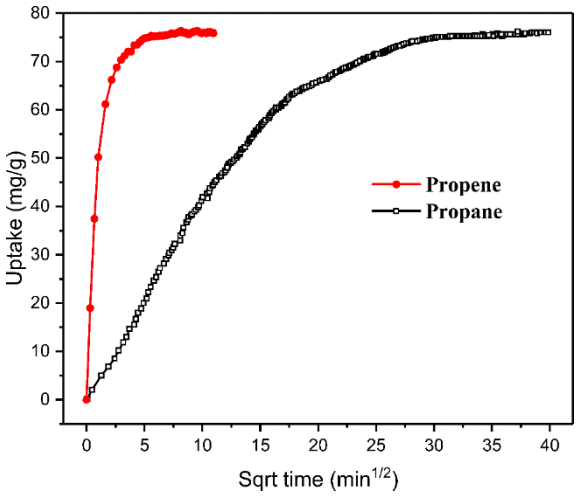

Fig. S11. Equilibrium propene and propane uptake in compound **1** as a function of square root of time at 363 K and 650 torr.

S11. Estimation of Pore Aperture/Window in Compounds 1 and 2

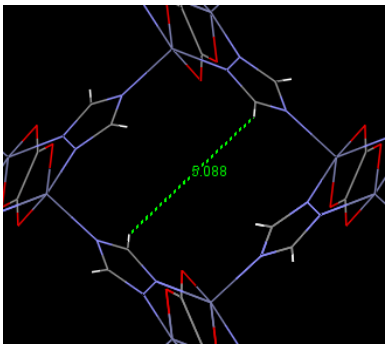

D(H-H) = 5.088-2rw(H) = 2.93Å

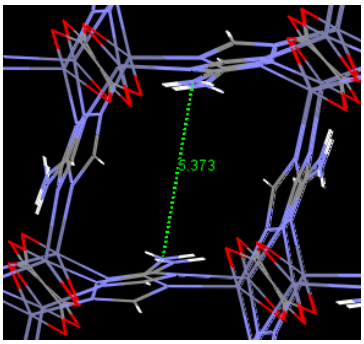

D(N-N) = 5.373-2rw(N) = 2.55Å

Fig. S12. The window sizes of **1** (left) and **2** (right) estimated by taking into account of van der Waals radii of H and N, respectively.

References

1. A. Banerjee, S. Nandi, P. Nasa and R. Vaidhyanathan, *Chemical Communications*, 2016, **52**, 1851-1854.
2. D. Banerjee, H. Wang, Q. Gong, A. M. Plonka, J. Jagiello, H. Wu, W. R. Woerner, T. J. Emge, D. H. Olson and J. B. Parise, *Chemical Science*, 2016, **7**, 759-765.
3. (a)H. S. Carslaw and J. C. Jaeger, *Oxford: Clarendon Press, 1959, 2nd ed.*, 1959; (b)C. Y. Lee, Y.-S. Bae, N. C. Jeong, O. K. Farha, A. A. Sarjeant, C. L. Stern, P. Nickias, R. Q. Snurr, J. T. Hupp and S. T. Nguyen, *Journal of the American Chemical Society*, 2011, **133**, 5228-5231.